Chin J Integr Med 2024 May;30(5):398-407

Chinese Journal of Integrative Medicine

Available online at link.springer.com/journal/11655
Journal homepage: www.cjim.cn/zxyjhen/zxyjhen/ch/index.aspx
E-mail: cjim_en@cjim.cn

Original Article

Mechanism of Qili Qiangxin Capsule for Heart Failure Based on miR133a-Endoplasmic Reticulum Stress*

JI Xiao-di[1,2], YANG Ding[1], CUI Xi-yuan[1], LOU Li-xia[1], NIE Bo[1], ZHAO Jiu-li[1], ZHAO Ming-jing[1], and WU Ai-ming[1]

ABSTRACT **Objective**: To investigate the pharmacological mechanism of Qili Qiangxin Capsule (QLQX) improvement of heart failure (HF) based on miR133a-endoplasmic reticulum stress (ERS) pathway. **Methods**: A left coronary artery ligation-induced HF after myocardial infarction model was used in this study. Rats were randomly assigned to the sham group, the model group, the QLQX group [0.32 g/(kg·d)], and the captopril group [2.25 mg/(kg·d)], 15 rats per group, followed by 4 weeks of medication. Cardiac function such as left ventricular ejection fraction (EF), fractional shortening (FS), left ventricular systolic pressure (LVSP), left ventricular end diastolic pressure (LVEDP), the maximal rate of increase of left ventricular pressure (+dp/dt max), and the maximal rate of decrease of left ventricular pressure (–dp/dt max) were monitored by echocardiography and hemodynamics. Hematoxylin and eosin (HE) and Masson stainings were used to visualize pathological changes in myocardial tissue. The mRNA expression of miR133a, glucose-regulated protein78 (GRP78), inositol-requiring enzyme 1 (IRE1), activating transcription factor 6 (ATF6), X-box binding protein1 (XBP1), C/EBP homologous protein (CHOP) and Caspase 12 were detected by RT-PCR. The protein expression of GRP78, p-IRE1/IRE1 ratio, cleaved-ATF6, XBP1-s (the spliced form of XBP1), CHOP and Caspase 12 were detected by Western blot. TdT-mediated dUTP nick-end labeling (TUNEL) staining was used to detect the rate of apoptosis. **Results**: QLQX significantly improved cardiac function as evidenced by increased EF, FS, LVSP, +dp/dt max, -dp/dt max, and decreased LVEDP ($P<0.05$, $P<0.01$). HE staining showed that QLQX ameliorated cardiac pathologic damage to some extent. Masson staining indicated that QLQX significantly reduced collagen volume fraction in myocardial tissue ($P<0.01$). Results from RT-PCR and Western blot showed that QLQX significantly increased the expression of miR133a and inhibited the mRNA expressions of GRP78, IRE1, ATF6 and XBP1, as well as decreased the protein expressions of GRP78, cleaved-ATF6 and XBP1-s and decreased p-IRE1/ IRE1 ratio ($P<0.05$, $P<0.01$). Further studies showed that QLQX significantly reduced the expression of CHOP and Caspase12, resulting in a significant reduction in apoptosis rate ($P<0.05$, $P<0.01$). **Conclusion**: The pharmacological mechanism of QLQX in improving HF is partly attributed to its regulatory effect on the miR133a-IRE1/XBP1 pathway.

KEYWORDS heart failure, Qili Qiangxin Capsule, miR133a, endoplasmic reticulum stress, apoptosis

Myocardial infarction (MI) has long been a serious cardiovascular event closely associated with heart failure (HF), causing an unacceptable number of deaths worldwide.[1] From a pathological point of view, HF post-MI is defined as myocardial cell death due to ischemic injury. Modern medicine has revealed the existence of multiple modes of cell death, including: apoptosis, necroptosis, mitochondrial permeability transition-driven necrosis, autophagy, pyroptosis, iron death, parthanatos, and so on.[2] These modes of cell death are highly regulated processes and vary according to the cellular environment and stimuli. Although there are multiple modes of cell death during HF after MI, a growing number of studies have shown that apoptosis plays an important role in cardiomyocyte loss.[3] Massive MI can cause billions of cardiomyocyte apoptosis, which are replaced by scar tissue.[4] This will lead to ventricular remodeling and impaired cardiac

*Supported by 2022 Science and Technology Innovation Project of Dongzhimen Hospital, Beijing University of Chinese Medicine (No. DZMKJCX-2022-008)

1. Dongzhimen Hospital Affiliated to Beijing University of Chinese Medicine, Key Laboratory of Chinese Internal Medicine of Ministry of Education and Beijing, Beijing (100700), China;
2. Department of Traditional Chinese Medicine, Fuwai Hospital, Chinese Academy of Medical Sciences & Peking Union Medical College, Beijing (100037), China
Correspondence to: Prof. WU Ai-ming, E-mail: wam688@163.com

DOI: https://doi.org/10.1007/s11655-024-3654-3

function, eventually developing into HF.

Endoplasmic reticulum stress (ERS), one of the major types of apoptosis induction, causes myocardial cell injury during HF post-MI due to excessive activation. Therefore, ERS is considered as one of the targets for the prevention and treatment of myocardial injury.[5] Recently, a study has found that miRNAs are involved in regulating excessive activation of ERS in the pathogenesis of HF.[6] They are a class of small non-coding RNAs which mediate the physiological and pathological processes of cardiovascular diseases by inhibiting the expression of target genes.[7] In particular, miR133a, one of the most abundant miRNAs in normal myocardial tissue, is involved in several biological processes, including cardiac growth, proliferation, and differentiation.[8] Overexpression of miR133a blocks apoptosis caused by myocardial hypoxia, and one of the mechanisms is regulating the ERS pathway.[9]

Although current medications can improve the symptoms of HF to some extent, they are inevitably accompanied by side effects with limited efficacy. However, Chinese medicine offers more options as complementary and alternative therapies for the treatment of HF due to its multi-component and multi-target properties. Qili Qiangxin Capsule (芪苈强心胶囊, QLQX), an herbal prescription composed of 11 herbs, has been widely applied in the treatment of clinical HF since it was approved by China Food and Drug Administration in 2004, with safety and efficiency.[10] Its chemical fingerprinting and compositional study ensure excellent quality control and stable active ingredients.[11] Previous studies have indicated that QLQX may exert myocardial protective effects by reducing inflammatory responses and oxidative stress, regulating energy metabolism, and mitigating ventricular remodeling.[12-14] Here, this study investigated the pharmacological mechanism of QLQX from the perspective of miR133a-ERS pathway.

METHODS

Animal Procedure

A total of 100 specific pathogen free (SPF) male Sprague-Dawley (SD) rats, 6 weeks, weighing (200±20) g, were acquired from Beijing Vital River Laboratory Animal Technology Co., Ltd. (License No. SCXK 2012-0001). The animals were housed in SPF animal experiment center at a constant temperature of 25±1 ℃ and humidity of 60%±10%, 12 h/12 h light and dark cycle. During feeding, the rats were given free access to deionized water and food. The animals used in this study have been approved by the Animal Management Committee of Dongzhimen Hospital of Beijing University of Chinese Medicine, with approval No.17-12. All animal work was carried out in accordance with the guidelines for laboratory animal care.

Animal Model and Administration

The rat model of HF was established by ligation of the left coronary artery (LCA) as described in the previous study.[15] The rats were anesthetized with 1% sodium pentobarbital (50 mg/kg). Then they were extubated and connected to a ventilator (DW3000-B, Beijing Jinyang Wanda Technology Co., Ltd., China). Subsequently, the chest cavity was opened and the LCA was ligated 2 mm below the inferior border between the pulmonary cone and the left auricle. The myocardial tissue below the ligation site become ischemic and turned white immediately, after which the chest was sutured layer by layer. The principle of asepsis was strictly followed throughout the operation. The same operation was performed on the sham group rats but without ligation. Finally, 40 U penicillin (lot No. F6062105, North China Pharmaceutical Co., Ltd., China) was injected intraperitoneally for 3 consecutive days to prevent infection.

According to the number of pathologic Q waves on electrocardiogram (ECG), a stratified random group assignment method was used to divide the surviving rats into 4 groups (15 rats per group): the sham group, the model group, the QLQX group, and the captopril group. QLQX was purchased from Shijiazhuang Yiling Pharmaceutical Co., Ltd. (lot No. A1612009, China), which consists of *Astragali Radix*, *Aconiti lateralis Radix praeparata*, *Ginseng radix et rhizome*, *Salviae miltiorrhizae radix et rhizome*, *Descurainiae semen lepidii semen*, *Alismatis rhizome*, *Polygonati odorati rhizome*, *Periplocae cortex*, *Citri reticulatae pericarpium*, *Cinnamomi ramulus*, *Carthami flos*. Fingerprint analysis showed a high reproducibility of the overall quality of QLQX, as reflected by the similarity of the medicine between the 10 batches in the range of 0.978 to 1.[16] QLQX from the same supplier as the above study was used in this experiment to ensure the quality control of this medicine. As a marketed Chinese patent medicine, the clinical dose of QLQX for adults is 0.056 g/(kg•d).[17] Acute toxicity tests in rats showed

Chin J Integr Med 2024 May;30(5):398-407

that QLQX was administered at a maximum dose of 32.73 g/(kg·d), that is, 584 times the clinical dose, and no mortality was observed in rats.[13] Several animal studies have shown that the drug exhibits efficacy and safety in the range of 0.25–1.2 g/(kg·d).[16.18.19] In this study, QLQX was administered at doses of 0.32g/(kg·d), equivalent to adult clinical dosage. Captopril Tablets were purchased from Sino-American Shanghai Squibb Pharmaceutical Co., Ltd. (lot No. AAN9869, China) and were administered at doses of 2.25mg/(kg·d). The sham group and the model group were given an equal volume of 10 mL/(kg·d) deionized water. Gavage administration was lasted for 4 consecutive weeks from the day after the operation.

Echocardiography

Ultrasound imaging system (Vevo 2100, Visual Sonics, Canada) was used to evaluate the function of the heart. Briefly, rats were anesthetized and fixed in the supine position, followed by acquisition of M-mode echocardiographic imaging of the heart under the guidance of a 15 MHz electronic wire-array probe for the purpose of calculating the left ventricular ejection fraction (EF) and fractional shortening (FS). Three consecutive cardiac cycles were collected from each rat.

Cardiac Hemodynamics

Left intraventricular intubation was used to monitor cardiac hemodynamics (BL-420, Chengdu Techman Software Co., Ltd., China). Rats were anesthetized by intraperitoneal injection of 1% sodium pentobarbital (45 mg/kg). After disinfection of the anterior cervical area, an incision of about 4 cm was made in the anterior cervical region to adequately expose the right common carotid artery. Carefully insert the catheter and advance it in the direction of the artery until it is inserted into the left ventricle. After the signal is stabilized, the following indicators are collected: left ventricular systolic pressure (LVSP), left ventricular end diastolic pressure (LVEDP), the maximal rate of increase of left ventricular pressure (+dp/dt max), the maximal rate of decrease of left ventricular pressure (–dp/dt max).

Histopathologic Staining

Hematoxylin eosin (HE) and Masson staining (lot No. D006 and D026, Nanjing Jiancheng Technology Co., Ltd., China) were used to visualize the extent of cardiac pathological damage and fibrosis by the following method: 4 μm slices were dewaxed with xylene and hydrated with gradient ethanol. Hematoxylin was used to stain the nucleus and eosin was used to stain the cytoplasm. Aniline blue was used to stain fiber tissues and then the collagen volume fraction (CVF) was calculated.

Real-Time PCR

Myocardial tissue was taken from the infarct margins and homogenized on ice. Then miRNA (lot No. 217004, QIAGEN Company, USA) and total RNA (lot No.15596026, Thermo Fisher Scientific, Inc., USA) were extracted according to the kit instructions, respectively. We ensured that OD260/OD280 values range from 1.8 to 2.0. The amplification conditions (GeneAmpPCR system 9700, Applied Biosystems, USA) were as follows: miR133a: pre-denaturation at 94 ℃ for 10 min, denaturation at 94 ℃ for 15 s, annealing at 60 ℃ for 60 s, extension at 72 ℃ for 10 s, a total of 45 cycles. The expression of miR133a were normalized to U6. Glucose-regulated protein 78 (GRP78), activating transcription factor 6 (ATF6), inositol-requiring enzyme 1 (IRE1), X-box binding protein1 (XBP1), C/EBP homologous protein (CHOP), Caspase 12: pre-denaturation at 95 ℃ for 10 min, denaturation at 95 ℃ for 30 s, annealing at 55 ℃ for 30 s, extension at 72 ℃ for 20 s, a total of 40 cycles. The expression of the above genes was normalized to GAPDH. The $2^{-\triangle\triangle CT}$ method was used to calculate relative expression The primer sequences were shown as follows (Table 1).

Table 1. The Sequences of All Primers

Gene	Primer sequences (5'-3')	Primer length (bp)
miR133a	F: 5'-ATGGTTCGTGCGTTTGGTCCCCTTCAACC -3'	29
	R: 5'-GCAGGGTCCGAGGTATTC -3'	18
U6	F: 5'-GCTTCGGCAGCACATATACTAAAAT -3'	25
	R: 5'-CGCTTCACGAATTTGCGTGTCAT -3'	23
GRP78	F: 5'-CCACCAGGATGCAGACATTG-3'	20
	R: 5'-AGGGCCTCCACTTCCATAGA-3'	20
ATF6	F: 5'-AGCACGTTCCTGAGGAGTTG-3'	20
	R: 5'-TTCCTTCAGTGGCTCTGCTG-3'	20
IRE1	F: 5'-GACCTACTACTGGCACGAGC-3'	20
	R: 5'-CAGAGATCAGGCCCATGGTC-3'	20
XBP1	F: 5'-GAGCAGCAAGTGGTGGATTT-3'	20
	R: 5'-AAGAGGCAACAGCGTCAGAAT-3'	21
CHOP	F: 5'-CCAGCAGAGGTCACAAGCAC-3'	20
	R: 5'-CGCACTGACCACTCTGTTTC-3'	20
Caspase 12	F: 5'-CACTGCTGATACAGATGAGG-3'	20
	R: 5'-CCACTCTTGCCTACCTTCC-3'	19
GAPDH	F: 5'-AGTTCAACGGCACAGTCAAG-3'	20
	R: 5'-TACTCAGCACCAGCATCACC-3'	20

Notes: F: forward, R: reverse

Western Blot

The myocardial tissue was homogenized in RIPA buffer (lot No. P0013B, Beyotime, China). Subsequently, the total protein concentration was determined by the bicinchoninic acid (BCA) kit (lot No. P0012, Beyotime, China). Proteins were separated in sodium dodecyl sulfate (SDS)-polyacrylamide gel (PAGE), and they were transferred to the nitrocellulose membrane, blocked with protein-free fast blocking buffer (lot No. PS108P, Shanghai YASE Biomedical Technology Co., Ltd., China). Then the membranes were incubated with GRP78 primary antibody (1:2000, lot No. 11587-1-AP, proteintech, USA), ATF6 primary antibody (1:1000, lot No. 24169-1-AP, proteintech, USA), IRE1 primary antibody (1:1000, lot No. DF7709, Affinity Biosciences, USA), phospho-IRE1 (Ser724) primary antibody (1:1000, lot No. AF7150, Affinity Biosciences, USA), XBP1 primary antibody (1:1000, lot No. AF5110, Affinity Biosciences, USA), CHOP primary antibody (1:1000, lot No. 15204-1-AP, proteintech, USA), Caspase 12 primary antibody (1:1000, lot No. 55238-1-AP, proteintech, USA) and GAPDH primary antibody (1:20,000, lot No. 10494-1-AP, proteintech, USA) respectively at 4 ℃ overnight. On the second day, the membrane was incubated with the corresponding secondary antibody for 1 h.

TdT-Mediated dUTP Nick-End Labeling Staining

TdT-mediated dUTP nick-end labeling (TUNEL) staining was used to assess the rate of apoptosis. According to the kit instructions (lot No. G3250, Promega, USA), the heart sections were immersed in immunostaining fixative (lot No. P0098, Beyotime, China) for 5 min, then the 20 μg/mL protease K solution was added onto the slices followed by re-fixation of the tissue. Next, the equilibration buffer and TdT reaction mix were added to the tissue and incubated, respectively. The reaction was terminated by adding termination solution. The number of apoptotic cell nuclei and normal cell nuclei were counted using Image-Pro Plus , with 8 replicates in each group, and the apoptosis rate was calculated.

Statistical Analysis

All data were statistically analyzed by SPSS 25.0 software (IBM Corp., USA). Measurement data were expressed as mean ± standard deviation ($\bar{x} \pm s$). Data in accordance with normal distribution were analyzed by one-way ANOVA. The LSD method was used for comparison between groups when the variance was equal, and Dunnett's T3 was used otherwise. $P<0.05$ was considered to be statistically significant.

RESULTS

Evidence of Successful Ligation of LCA in Rats

ECG results showed that both groups of rats were in the normal range before the operation. Compared with the sham group, the LCA-ligated rats showed ST-segment elevation on the ECG immediately after the operation and pathological Q waves appeared on the ECG 24 h after the operation, suggesting myocardial injury.

Meanwhile, the gross cardiac structure 4 weeks after the operation showed that the hearts of the sham group were structurally intact with red myocardial tissue. While the hearts of rats in the model group exhibited prominent infarcted areas that were whitened due to myocardial ischemia injury and partially replaced by fibrotic tissue.

Echocardiographic results showed that 4 weeks after LCA ligation, left ventricular EF and FS were significantly reduced in the model group ($P<0.01$), suggesting the successful establishment of a rat model of HF after MI (Figure 1).

QLQX Improves Cardiac Function in Rats with HF Post-MI

The results showed that LVSP, +dp/dt max, and –dp/dt max were significantly decreased, while LVEDP was significantly increased in the model group of rats compared with the sham group ($P<0.01$). Compared with the model group, LVSP, +dp/dt max, and –dp/dt max were significantly increased and LVEDP was significantly decreased in the QLQX group and the captopril group ($P<0.05$, $P<0.01$, Figure 2).

QLQX Improves Myocardial Tissue Morphology in Rats with HF Post-MI

HE staining showed that there was no obvious histological change in myocardial tissue in the sham group, which was reflected in the clear horizontal stripes dense and neat arrangement, and complete structure of myocardial fibers. In the model group, obvious cell degeneration, necrosis, rupture of myocardial fibers, hypertrophy of remaining myocardial cells, and pyknosis were observed in the infarct border of myocardial tissue. However, compared with the model group, the cell morphology of the QLQX and captopril group

Chin J Integr Med 2024 May;30(5):398-407

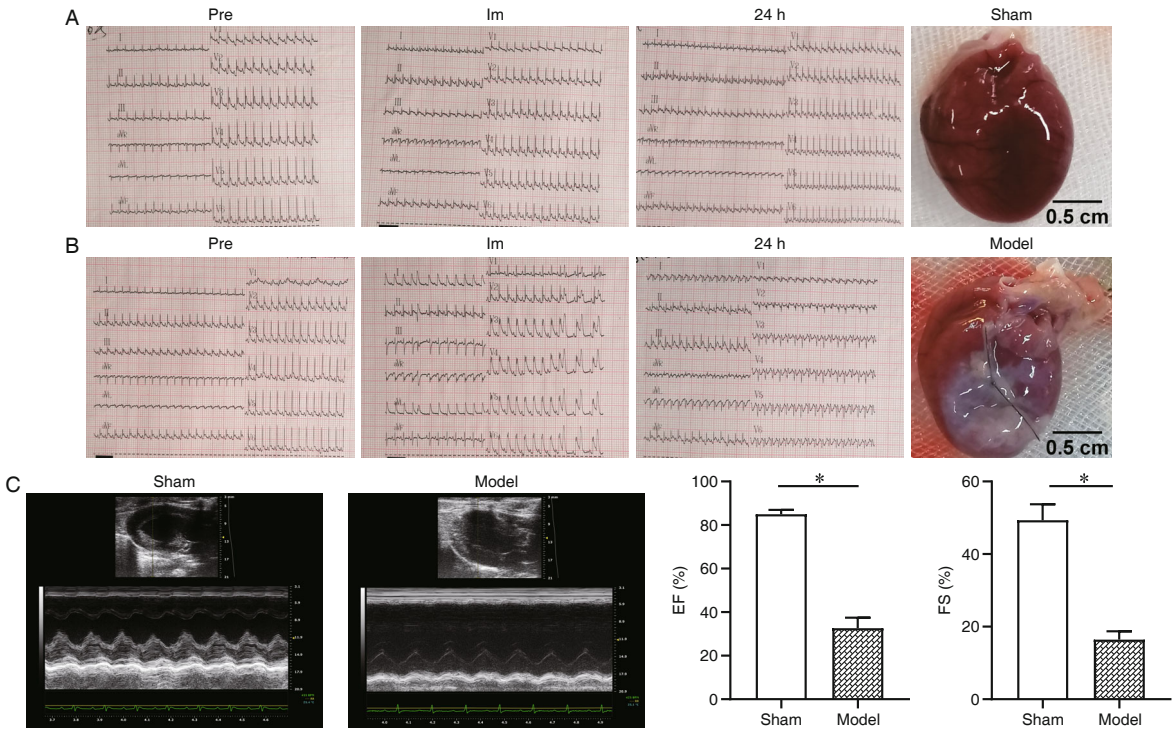

Figure 1. Cardiac Function Changes in Rats with Ligation of Left Coronary Artery Anterior Descending Branches

Notes: Electrocardiogram and gross structure of rats without ligation (A) and with ligation (B) of the left coronary artery anterior descending branch. (C) Cardiac function measured by echocardiography. Pre: before the operation; Im: immediately after the operation; 24 h: 24 h after the operation. EF: ejection fraction; FS: fractional shortening. The data of bur graph are presented as $\bar{x} \pm s$, n=8 per group. $^{*}P$<0.01

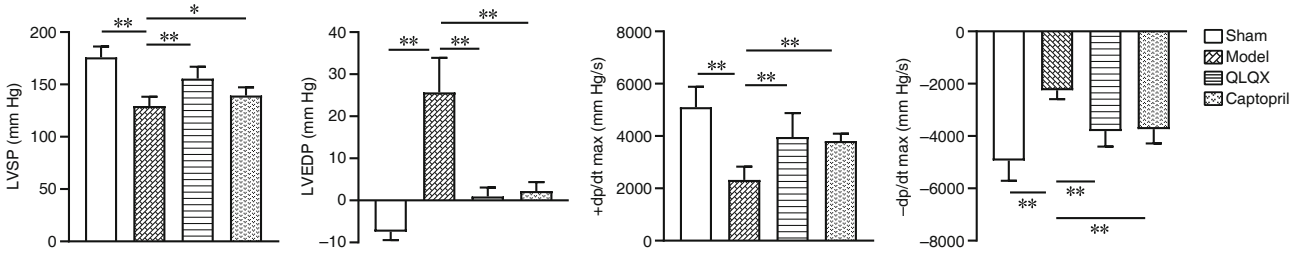

Figure 2. Effect of QLQX on Cardiac Hemodynamics in Rats with HF Post-MI ($\bar{x} \pm s$, n=8)

Notes: LVSP: left ventricular systolic pressure; LVEDP: left ventricular end diastolic pressure; +dp/dt max: the maximal rate of increase of left ventricular pressure; −dp/dt max: the maximal rate of decrease of left ventricular pressure. $^{*}P$<0.05, $^{**}P$<0.01

was basically the same, showing that the structure of myocardial cells was significantly improved, and histopathological changes were alleviated (Figure 3).

QLQX Improves Collagen Deposition in Myocardial Tissue of Rats with HF Post-MI

As shown in Figure 4, the nucleus was stained to blue-purple, the cytoplasm was stained to red, and the interstitial collagen fibers were stained to blue. There were basically no blue collagen fibers in the myocardial tissue of the sham group. Compared with the sham group, a large number of blue collagen fibers occupied the myocardial tissue, and the CVF was significantly increased in the model group (P<0.01), with the characteristics of fibrosis. Compared with the model group, the collagen content decreased in the

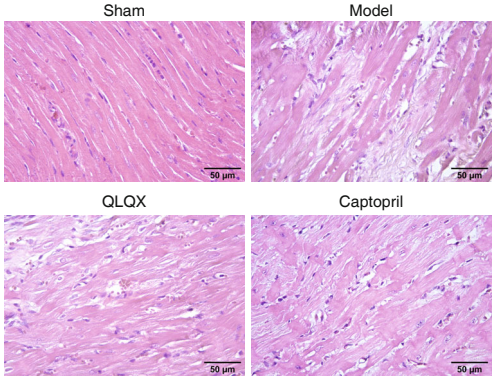

Figure 3. Representative Image of Hematoxylin Eosin Staining of Myocardial Tissue

Note: The scale bar is 50 μm (40×)

QLQX group and the captopril group (P<0.01), the degree of fibrosis was alleviated.

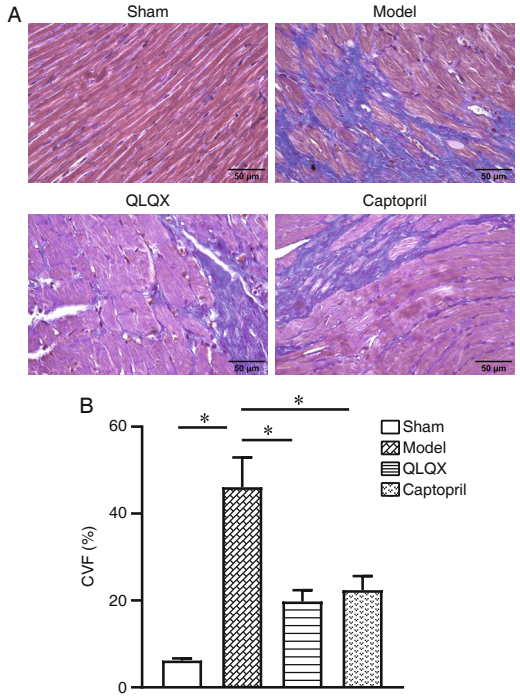

Figure 4. Effect of QLQX on Cardiac Collagen Deposition in Rats with HF Post-MI

Notes: (A) Representative image of Masson staining of myocardial tissue, the scale bar is 50 μm (40×); (B) Statistical analysis of myocardial collagen volume fraction. CVF: collagen volume fraction. Data are presented as $\bar{x} \pm s$, n=4 per group. *P<0.01

Regulatory Effect of QLQX on miR133a and Expression of ERS Pathway Molecules in Rats with HF Post-MI

The expression of miR133a was significantly reduced in the model group compared with the sham group. QLQX and captopril significantly increased the expression of miR133a compared with the model group (P<0.01, Figure 5A).

There was obvious ERS in the model group, as evidenced by significantly elevated mRNA expression of GRP78, IRE1, ATF6, and XBP1, as well as significantly enhanced protein expression of GRP78, p-IRE1/IRE1 ratio, cleaved-ATF6, and XBP1-s (the spliced form of XBP1, P<0.05, P<0.01). QLQX intervention dramatically inhibited the expression of these molecules at the mRNA and protein levels (P<0.05, P<0.01, Figures 5B and 5C).

Regulatory Effect of QLQX on Apoptosis in Rats with HF Post-MI

The RT-PCR results indicated that compared with the sham group, the mRNA expression of CHOP and Caspase 12 in model group were significantly increased (P<0.01). While compared with the model group, their mRNA expression levels in the QLQX group and captopril group were significantly decreased (P<0.05, P<0.01). Western blot revealed that compared with the sham group, the protein expression of CHOP and Caspase 12 in the model group was significantly increased (P<0.01), QLQX significantly reduced their protein expression (P<0.05, P<0.01). The protein expression of CHOP was significantly declined in the captopril group (P<0.01), while the protein expression of Caspase 12 only tended to decrease (P>0.05, Figures 6A and 6B).

As TUNEL staining results showed in Figure 6C, green fluorescence represents broken DNA strands, that is apoptotic cells; blue fluorescence represents all nuclei. There were few apoptotic cells seen in the sham group, while the number of apoptotic cells was

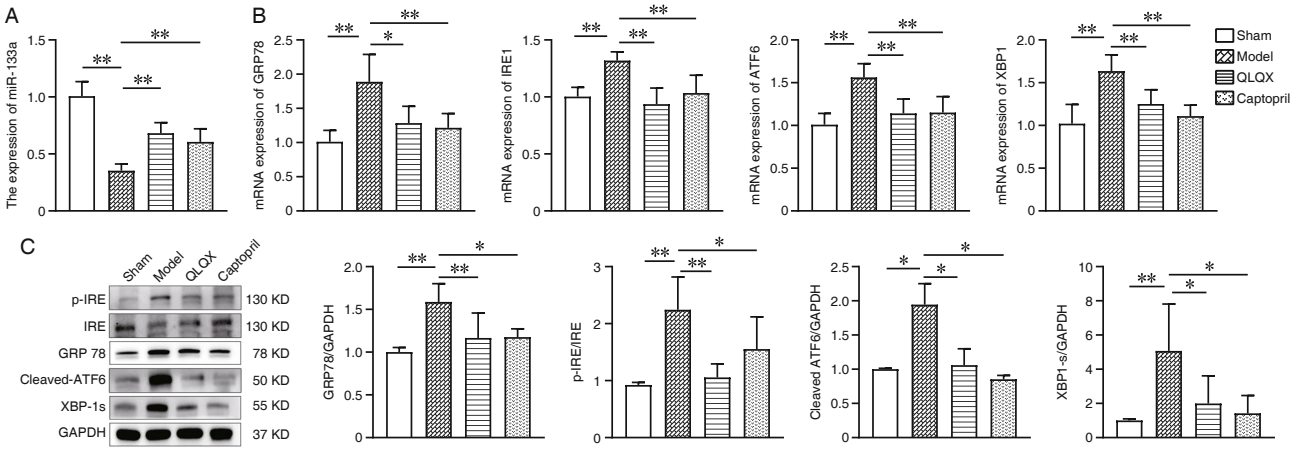

Figure 5. Effect of QLQX on miR133a-ERS Pathway in Rats with HF Post-MI

Notes: (A) The expression of miR133a was detected by RT-PCR (n=8); (B) The mRNA expression of GRP78, IRE1, ATF6 and XBP1 was detected by RT-PCR (n=8); (C) The protein expression of GRP78, p-IRE1, IRE1, cleaved-ATF6, and XBP1-s was detected by Western blot (n=4). ERS: endoplasmic reticulum stress; GRP78: glucose-regulated protein78; IRE1: inositol-requiring enzyme 1; ATF6: a ctivating transcription factor 6; XBP1: X-box binding protein 1. Data are presented as $\bar{x} \pm s$. *P<0.05, **P<0.01

Chin J Integr Med 2024 May;30(5):398-407

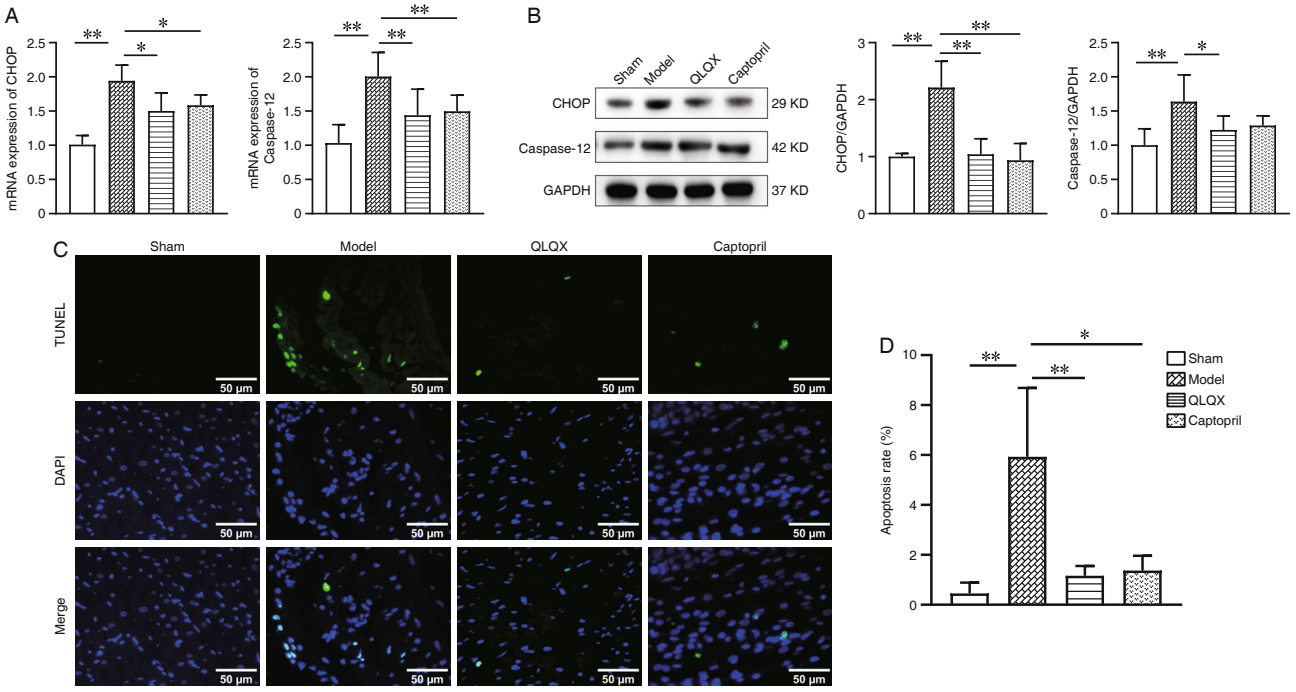

Figure 6. Effect of QLQX on Apoptosis in Rats with HF Post-MI

Notes: (A) The mRNA expression of CHOP and Caspase 12 was detected by RT-PCR (n=8). (B) The protein expression of CHOP and Caspase 12 was detected by Western Blot (n=4). (C) Representative image of TUNEL staining of myocardial tissue. The scale bar is 50 μm (40×). (D) Effect of QLQX on myocardial apoptosis rate (n=8). CHOP: C/EBP homologous protein; TUNEL:TdT-mediated dUTP nick-end labeling. Data are presented as $\bar{x} \pm s$. $^{*}P<0.05$, $^{**}P<0.01$

significantly increased in the model group, which showed the rate of apoptosis was significantly increased ($P<0.01$). This was markedly decreased in QLQX group and captopril group ($P<0.05$, $P<0.01$, Figure 6D).

DISCUSSION

HF, the end stage of many cardiovascular diseases including MI, has an overall poor prognosis with a 5-year survival rate of no more than 50%. Despite some clinical advances in both pharmacologic and non-pharmacologic treatments for HF, its mortality rate has not improved. Therefore, finding effective ways to treat HF remains a major issue in the cardiovascular field. Chinese medicine has centuries of history and practical experience in the treatment of cardiovascular diseases, and has demonstrated great advantages and potential in improving HF after MI.[20] QLQX is a marketed proprietary Chinese medicine consisting of 11 herbs, demonstrating excellent cardioprotective effects in the clinical treatment of HF.[21] However, the mechanism of this medicine has not been fully elucidated.

In recent years, miRNAs have shown tremendous promise in the treatment of HF. Myocardial ischemia induced changes in the expression of some miRNAs, especially miR133a. Previous literature suggests that some transcription factors such as myocyte enhancer factor 2, serum response factor, etc. can bind to the miR133a promoter region and thus regulate its expression.[22,23] In addition, some signaling pathways such as Wnt and histone deacetylases can act on transcriptional regulators of miR133a to regulate its nuclear localization. Further, some non-coding RNAs have also been found to regulate the expression of miR133a.[24-26] During myocardial hypoxia, miR133a inhibition is involved in cardiomyocyte apoptosis. Upregulation of miR133a protects cardiomyocytes against apoptosis.[27] At the same time, ERS is overactivated during myocardial hypoxia, which in turn induces apoptosis.[28] One study found that overexpression of miR133a inhibited overactivated ERS, which in turn reduced cardiomyocyte apoptosis, and anti-miR133a treatment resulted in significant ERS activation in cardiomyocytes during hypoxia.[29,30] However, whether the pharmacological mechanism of QLQX to improve HF is related to the miR133a-ERS pathway has not yet been reported. Thus, this study proposed the hypothesis that QLQX regulated the miR133a-ERS pathway and protected the heart.

To begin with, the echocardiographic and hemodynamic results suggested that QLQX

significantly strengthened cardiac function. Then, we focused on the mechanisms by which it exerted its efficacy. ERS, occurring in myocardial cell due to ischemia and hypoxia during HF, is characterized by the accumulation of large amounts of unfolded/misfolded proteins in the endoplasmic reticulum (ER). As the chaperone of the ER, GRP78 plays a crucial part in maintaining its homeostasis and is the marker of ERS.[30] This investigation showed that QLQX significantly increased the expression of miR133a and, at the same time, inhibited the expression of mRNA and protein of GRP78 in heart. This suggested that miR133a-ERS pathway was the potential target for QLQX to exert cardioprotective effects.

To investigate the specific role of QLQX in regulating ERS, we observed changes in its pathway proteins. Under physiological state, GRP78 binds to the 3 sensors on the ER membrane, IRE1, ATF6, and protein kinase RNA-like ER kinase (PERK) to make them inactive.[32] During ERS, GRP78 binds to unfolded/misfolded proteins, releasing IRE1, ATF6, and PERK, which in turn activate the unfolded protein response (UPR). Among 3 signaling pathways of the UPR, it is the IRE1 pathway that is the most conserved and sensitive, involved in a variety of pathological processes and determines the fate of cells: survival or apoptosis.[33] Once UPR activation, IRE1 instantly oligomerizes and autophosphorylates in its RNase domain, which leads to the activation of its endoribonuclease activity. This activation of the IRE1 enables it to splice XBP1 into active XBP1-s, which in turn translocates to the nucleus to regulate UPR target genes.[34] Note that XBP1 mRNA was induced by ATF6.[35] In the present study, we observed that QLQX significantly reduced the expression of mRNA for IRE1, XBP1, and ATF6 as well as the expression of proteins for p-IRE1/ IRE1, XBP1-s, and ATF6 during HF. This suggested that QLQX could target the IRE1/XBP1 pathway to regulate ERS.

It's worth noting that moderate UPR can exert a protective effect by enhancing the ability of the ER to cope with unfolded/misfolded proteins, whereas during HF, UPR tends to be sustained and excessive, which can trigger apoptotic signaling and followed by promoting cellular damage and ventricular remodeling. CHOP and Caspase 12 are key proteins in ERS-induced apoptosis. Our results showed that QLQX significantly inhibited the expression of CHOP and Caspase12. TUNEL staining suggested that QLQX reduced the rate of cardiomyocyte apoptosis. In addition, Masson staining suggested that QLQX decreased myocardial collagen deposition. During myocardial ischemia, on the one hand, apoptosis induces an inflammatory response and myofibroblast activation, which promotes the fibrosis process; on the other hand, myocardial fibrosis releases some signaling molecules that promote cardiomyocyte apoptosis.[36] Myocardial apoptosis and fibrosis regulate each other, ultimately resulting in ventricular remodeling. In this study, QLQX both modulated apoptosis and ameliorated fibrosis, which benefited cardiac function.

There are some limitations to this study. Firstly, captopril, an angiotensin-converting enzyme inhibitor (ACEI), has been shown to reduce myocardial fibrosis and apoptosis. This medication is often used alone as a positive control group in basic studies of HF.[37] However, modern medicine advances very fast in treating HF post MI, multidrug combinations of diuretics, ACEI or angiotensin receptor blockers or angiotensin receptor–neprilysin inhibitors, mineralocorticoid receptor antagonists, sodium–glucose co-transporter, and beta-blocker are a clinical strategy for the treatment of HF.[38] Thus, the use of captopril alone as a positive control group is limiting, and strategies that mimic clinical combinations of medications are the direction for future refinement of basic research. Secondly, the question of how QLQX and captopril regulate miR133a is not explored in depth in this study. QLQX may regulate miR133a expression in the nucleus by regulating transcription factors or non-coding RNAs, or it may indirectly affect miR133a expression by acting on some signaling pathways in the cytoplasm, which are worthy to be further explored in the next studies.

Taken together, this study showed that QLQX administration effectively improved cardiac function. The pharmacological mechanism was to modulate the miR133a-IRE1/XBP1 pathway, which in turn alleviated over-activated ERS during HF (Figure 7).

Conflict of Interest

The authors declare that they have no conflicts of interest.

Author Contributions

Wu AM designed the general study and revised the manuscript. Zhao MJ guided the manuscript writing ideas as well as provided important advice on the experimental design.

Chin J Integr Med 2024 May;30(5):398-407

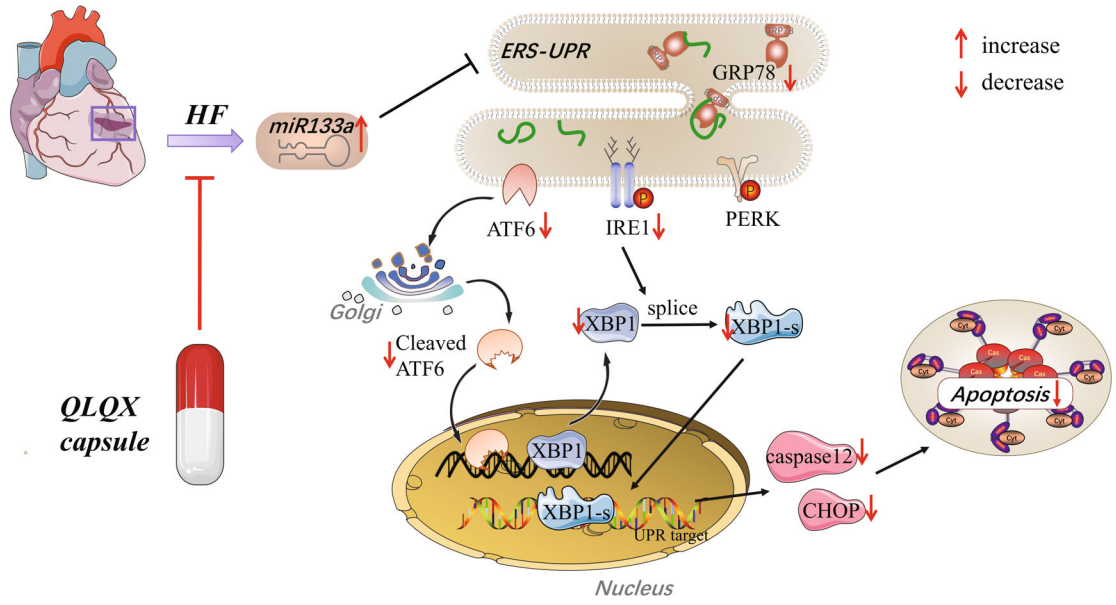

Figure 7. Regulatory Mechanisms of QLQX to Alleviate HF Post-MI

Lou LX, Nie B and Zhao JL provided guidance on experimental techniques. Ji XD and Yang D detected the experimental indicators. Cui XY searched the literature. Ji XD wrote the manuscript as well as drew the mechanism chart. All authors reviewed and agreed to submit the final manuscript.

Data Availability

The data used to support the findings of this study are available from the corresponding author upon request.

REFERENCES

1. Virani SS, Alonso A, Aparicio HJ, Benjamin EJ, Bittencourt MS, Callaway CW, et al. Heart disease and stroke statistics—2021 update: a report from the american heart association. Circulation 2021;143:e254-e743.
2. Martens MD, Karch J, Gordon JW. The molecular mosaic of regulated cell death in the cardiovascular system. Biochim Biophys Acta Mol Basis Dis 2022;1868:166297.
3. Wang Q, Zhou H, Zhu X, Jiang F, Yu Q, Zhang J, et al. miR-208 inhibits myocardial tissues apoptosis in mice with acute myocardial infarction by targeting inhibition of PDCD4. J Biochem Mol Toxicol 2022;36:e23202.
4. Frantz S, Hundertmark MJ, Schulz-Menger J, Bengel FM, Bauersachs J. Left ventricular remodelling post-myocardial infarction: Pathophysiology, imaging, and novel therapies. Eur Heart J 2022;43:2549-2561.
5. Lin R, Su Z, Tan X, Su Y, Chen Y, Shu X, et al. Effect of endoplasmic reticulum stress and autophagy in the regulation of post-infarct cardiac repair. Arch Med Res 2018;49:576-582.
6. Fan M, Zhang J, Zeng L, Wang D, Chen J, Xi X, et al. Non-coding RNA mediates endoplasmic reticulum stress-induced apoptosis in heart disease. Heliyon 2023;9:e16246.
7. Tual-Chalot S, Stellos K. microRNA-based therapy of postmyocardial infarction heart failure. Hellenic J Cardiol 2021;62:149-151.
8. Puthanveetil P, O'hagan KP. miR-133a-A potential target for improving cardiac mitochondrial health and regeneration after injury. J Cardiovasc Pharmacol 2022;80:187-193.
9. Yang H, He X, Wang C, Zhang L, Yu J, Wang K. Knockdown of tug 1 suppresses hypoxia-induced apoptosis of cardiomyocytes by up-regulating miR-133a. Arch Biochem Biophys 2020;681:108262.
10. Li X, Zhang J, Huang J, Ma A, Yang J, Li W, et al. A multicenter, randomized, double-blind, parallel-group, placebo-controlled study of the effects of Qili Qiangxin Capsules in patients with chronic heart failure. J Am Coll Cardiol 2013;62:1065-1072.
11. Tang XY, Dai ZQ, Zeng JX, Li ZT, Fan CL, Yao ZH, et al. Pharmacokinetics, hepatic disposition, and heart tissue distribution of 14 compounds in rat after oral administration of Qi-li-qiang-xin Capsule via ultra-high-performance liquid chromatography coupled with triple quadrupole tandem mass spectrometry. J Sep Sci 2022;45:2177-2189.
12. Zhao Q, Li H, Chang L, Wei C, Yin Y, Bei H, et al. Qili Qiangxin attenuates oxidative stress-induced mitochondrion-dependent apoptosis in cardiomyocytes via PI3K/AKT/GSK3β signaling pathway. Biol Pharm Bull 2019;42:1310-1321.
13. Cheng W, Wang L, Yang T, Wu A, Wang B, Li T, et al. Qili Qiangxin Capsules optimize cardiac metabolism flexibility in rats with heart failure after myocardial infarction. Front Physiol 2020;11:805.
14. Lu Y, Xiang M, Xin L, Zhang Y, Wang Y, Shen Z, et al.

Qili Qiangxin modulates the gut microbiota and NLRP3 inflammasome to protect against ventricular remodeling in heart failure. Front Pharmacol 2022;13:905424.
15. Yang W, Zhang A, Han Y, Su X, Chen Y, Zhao W, et al. Cyclin-dependent kinase inhibitor 2b controls fibrosis and functional changes in ischemia-induced heart failure via the BMI1-p15-rb signalling pathway. Can J Cardiol 2021;37:655-664.
16. Zhang J, Wei C, Wang H, Tang S, Jia Z, Wang L, et al. Protective effect of Qili Qiangxin Capsule on energy metabolism and myocardial mitochondria in pressure overload heart failure rats. Evid Based Complement Alternat Med 2013;2013:378298.
17. Leung AYL, Chen H, Jia Z, Li X, Shen J. Study protocol: traditional Chinese medicine syndrome differentiation for heart failure patients and its implication for long-term therapeutic outcomes of the Qili Qiangxin Capsules. Chin Med 2021;16:103.
18. Fan C, Tang X, Ye M, Zhu G, Dai Y, Yao Z, et al. Qi-li-qiang-xin alleviates isoproterenol-induced myocardial injury by inhibiting excessive autophagy via activating akt/mtor pathway. Front Pharmacol 2019;10:1329.
19. Tao L, Shen S, Fu S, Fang H, Wang X, Das S, et al. Traditional Chinese medication Qili Qiangxin attenuates cardiac remodeling after acute myocardial infarction in mice. Sci Rep 2015;5:8374.
20. Hu YX, Qiu SL, Shang JJ, Wang Z, Lai XL. Pharmacological effects of botanical drugs on myocardial metabolism in chronic heart failure. Chin J Integr Med 2023 [Epub ahead of print].
21. Xu XM, Yang Y, Zhou GD, Du ZX, Zhang XH, Mao W, et al. Clinical efficacy of Qili Qiangxin capsule combined with western medicine in the treatment of chronic heart failure: a systematic review and meta-analysis. Evid-Based Complementary Alternat Med 2021;2021.
22. Zhang X, Azhar G, Helms SA, Wei JY. Regulation of cardiac microRNAs by serum response factor. J Biomed Sci 2011;18:15.
23. Mughal W, Nguyen L, Pustylnik S, Da Silva Rosa SC, Piotrowski S, Chapman D, et al. A conserved mads-box phosphorylation motif regulates differentiation and mitochondrial function in skeletal, cardiac, and smooth muscle cells. Cell Death Dis 2015;6:e1944.
24. Di Mauro V, Crasto S, Colombo FS, Di Pasquale E, Catalucci D. Wnt signalling mediates miR-133a nuclear re-localization for the transcriptional control of DNMT3b in cardiac cells. Sci Rep 2019;9:9320.
25. Renaud L, Harris LG, Mani SK, Kasiganesan H, Chou JC, Baicu CF, et al. HDACs regulate miR-133a expression in pressure overload-induced cardiac fibrosis. Circ Heart Fail 2015;8:1094-1104.
26. Si X, Zheng H, Wei G, Li M, Li W, Wang H, et al. CircRNA HIPK3 induces cardiac regeneration after myocardial infarction in mice by binding to notch1 and miR-133a. Mol Ther Nucleic Acids 2020;21:636-655.
27. Li S, Xiao FY, Shan PR, Su L, Chen DL, Ding JY, et al. Overexpression of microRNA-133a inhibits ischemia-reperfusion-induced cardiomyocyte apoptosis by targeting DAPK2. J Hum Genet 2015;60:709-716.
28. Qu Y, Gao R, Wei X, Sun X, Yang K, Shi H, et al. Gasdermin D mediates endoplasmic reticulum stress via FAM134b to regulate cardiomyocyte autophagy and apoptosis in doxorubicin-induced cardiotoxicity. Cell Death Dis 2022;13:901.
29. Ren L, Wang Q, Chen Y, Ma Y, Wang D. Involvement of microRNA-133a in the protective effect of hydrogen sulfide against ischemia/reperfusion-induced endoplasmic reticulum stress and cardiomyocyte apoptosis. Pharmacology 2019;103:1-9.
30. Feng J, Li S, Chen H. Tanshinone ⅡA ameliorates apoptosis of cardiomyocytes induced by endoplasmic reticulum stress. Exp Biol Med (Maywood) 2016;241:2042-2048.
31. Yang FW, Fu Y, Li Y, He YH, Mu MY, Liu QC, et al. Prostaglandin E1 protects hepatocytes against endoplasmic reticulum stress-induced apoptosis via protein kinase A-dependent induction of glucose-regulated protein 78 expression. World J Gastroenterol 2017;23:7253-7264.
32. Martinez-Amaro FJ, Garcia-Padilla C, Franco D, Daimi H. LncRNAs and circRNAs in endoplasmic reticulum stress: A promising target for cardiovascular disease? Int J Mol Sci 2023;24:9888.
33. Adams CJ, Kopp MC, Larburu N, Nowak PR, Ali MMU. Structure and molecular mechanism of ER stress signaling by the unfolded protein response signal activator IRE1. Front Mol Biosci 2019;6:11.
34. Luo X, Alfason L, Wei M, Wu S, Kasim V. Spliced or unspliced, that is the question: the biological roles of XBP1 isoforms in pathophysiology. Int J Mol Sci 2022;23:2746.
35. Mondal A, Burchat N, Sampath H. Palmitate exacerbates bisphenol a toxicity via induction of ER stress and mitochondrial dysfunction. Biochim Biophys Acta Mol Cell Biol Lipids 2021;1866:158816.
36. Frangogiannis NG. Transforming growth factor-β in myocardial disease. Nat Rev Cardiol 2022;19:435-455.
37. Chai R, Ye Z, Xue W, Shi S, Wei Y, Hu Y, et al. Tanshinone ⅡA inhibits cardiomyocyte pyroptosis through TLR4/NF-κB p65 pathway after acute myocardial infarction. Front Cell Dev Biol 2023;11:1252942.
38. Mcdonagh TA, Metra M, Adamo M, Gardner RS, Baumbach A, Böhm M, et al. 2023 Focused update of the 2021 ESC guidelines for the diagnosis and treatment of acute and chronic heart failure. Eur Heart J 2023;44:3627-3639.

(Accepted November 27, 2023; First Online February 22, 2024)
Edited by ZHANG Wen